

# Order parameter for two-dimensional critical systems with boundaries

Ivica Reš and Joseph P. Straley

*Department of Physics and Astronomy, University of Kentucky, Lexington, KY 40506-0055*

Conformal transformations can be used to obtain the order parameter for two-dimensional systems at criticality in finite geometries with fixed boundary conditions on a connected boundary. To the known examples of this class (such as the disk and the infinite strip) we contribute the case of a rectangle. We show that the order parameter profile for simply connected boundaries can be represented as a universal function (independent of the criticality model) raised to the power  $\frac{1}{2}\eta$ . The universal function can be determined from the Gaussian model or equivalently a problem in two-dimensional electrostatics. We show that fitting the order parameter profile to the theoretical form gives an accurate route to the determination of  $\eta$ . We perform numerical simulations for the Ising model and percolation for comparison with these analytic predictions, and apply this approach to the study of the planar rotor model.

PACS numbers: 64.60.Cn, 05.70.Jk, 64.60.Fr

## I. INTRODUCTION

A system undergoing a continuous phase transition is scale invariant at its critical point. An interesting and productive generalization of this idea for systems also having translational and rotational invariance is to assume conformal invariance [1,2]. Among other things, this implies that the magnetization (the one-point correlation function) for a two-dimensional critical system transforms under a conformal transformation  $w = w(z)$  in the following way:

$$\langle \phi(w, \bar{w}) \rangle = \left(\frac{dw}{dz}\right)^{-h} \left(\frac{d\bar{w}}{d\bar{z}}\right)^{-\bar{h}} \langle \phi(z, \bar{z}) \rangle. \quad (1)$$

Here  $\langle \rangle$  means the statistical average,  $z = x + iy$  is a complex-valued coordinate, and it is assumed that  $\langle \phi(z, \bar{z}) \rangle$  is nonzero due to a breaking of the  $\phi$  field symmetry at a boundary. For a spinless field  $\phi$ , the scaling exponent  $\Delta$  is related to the conformal dimension  $h$  through the relations

$$h = \bar{h} = \frac{1}{2}\Delta, \quad (2)$$

and to the correlation exponent  $\eta$  by

$$\Delta = \frac{1}{2}\eta. \quad (3)$$

Specific values for  $\eta$  relevant to what follows are [3]  $\eta = \frac{1}{4}$  for the Ising model and  $\eta = \frac{5}{24}$  for percolation.

In this paper we consider a system at its critical point in a domain, with fixed boundary conditions on the boundary. Examples of the model system we have in mind would be the magnetization  $m(x, y)$  of the Ising model at its critical temperature defined on the half-plane  $(x, y > 0)$ , with the spins on the boundary  $y = 0$  kept at the value of  $+1$ , or a percolating system at threshold, where  $m(x, y)$  is the probability that the site  $(x, y)$  is connected to the boundary  $y = 0$ . We will describe the models in this way, even though we will mostly be considering the continuum versions of the theories, for which the boundary condition is that the field is fixed at  $\phi \rightarrow \infty$  at the boundary. For the half-plane geometry, the form of the magnetization is fixed by translational, rotational, and scale invariance

$$\langle m(x, y) \rangle = Cy^{-\Delta}, \quad (4)$$

where  $C$  is a constant. This result also describes the behavior of a lattice model, except when  $y$  is as small as a few lattice spacings; the different behavior at short distances can be viewed as the consequence of corrections to scaling, which in any case are missing from Eq. (4). Eq. (1) is relevant to a more general problem, because it relates the profiles for different-shaped regions; this has been used [4] to determine the magnetization profile for several cases, such as the disk and the infinite strip.

As will be shown below, conformal invariance implies that the critical magnetization profiles for *different* models can be expressed in terms of a single function  $m_1(\vec{r})$ :

$$m(\vec{r}) = m_1(\vec{r})^\Delta, \quad (5)$$

where  $m_1(\vec{r})$  is a function that depends on the shape of the domain but not on any feature of the model, and describes the critical behavior of a mythical model with  $\Delta = 1$ . The meaning of this result is that all conformally invariant models with the same exponent  $\Delta$  have the same magnetization profile; then it is enough to look at the magnetization profile for the Gaussian models. Therefore, Section 2 will begin with a discussion of the Gaussian model and end with the proof of the assertion (5), and with explicit exhibition of the function  $m_1$  for some simple geometries.

Section 3 will present some numerical simulations for the Ising and percolation models, verifying that they are related this way and showing that fitting the numerical data to the known form of  $m_1$  gives an accurate way to determine  $\Delta$ , in which far from worrying about the implications of boundaries and finite size, we are *making use* of their known effects.

In Section 4 we will demonstrate the usefulness of this technique in a determination of the temperature dependence of  $\eta$  for the planar spin model.

## II. ORDER PARAMETER PROFILE IN FINITE GEOMETRIES ACCORDING TO THE GAUSSIAN MODEL

The Gaussian model has the action

$$S = \frac{1}{2}g \int |\vec{\nabla}\theta|^2 d^2r. \quad (6)$$

The order parameter is

$$m(\vec{r}) = Re < e^{i\theta(\vec{r})} >, \quad (7)$$

where the expectation value can be evaluated from the functional integral

$$m(\vec{r}) = \frac{Re \int e^{i\theta(\vec{r})} e^{-S} \mathcal{D}\theta}{\int e^{-S} \mathcal{D}\theta}. \quad (8)$$

To calculate this integral we expand the field  $\theta$  in terms of a set of functions  $\varphi_\lambda$

$$\theta(\vec{r}) = \sum_\lambda \alpha_\lambda \varphi_\lambda(\vec{r}), \quad (9)$$

and treat the coefficients  $\alpha_\lambda$  as independent degrees of freedom. The boundary condition on spin ordering becomes the condition that  $\varphi_\lambda(\vec{r})$  takes a constant value (zero, for the moment) for  $\vec{r}$  on the boundary. It proves useful to choose these functions to be the normalized eigenfunctions  $\varphi_\lambda$  of the Laplacian

$$-\nabla^2 \varphi_\lambda(\vec{r}) = \lambda \varphi_\lambda(\vec{r}), \quad (10)$$

because these diagonalize the action; the resulting Gaussian integrals give

$$m(\vec{r}) = e^{-\frac{1}{2g} \sum_\lambda \lambda^{-1} \theta_\lambda^2(\vec{r})}. \quad (11)$$

Interpretation of this result is facilitated by the observation that the two-point function

$$G(\vec{R}, \vec{r}) = \sum_\lambda \frac{1}{\lambda} \varphi_\lambda(\vec{R}) \varphi_\lambda(\vec{r}), \quad (12)$$

is the Dirichlet Green function: it satisfies

$$-\nabla_{\vec{R}}^2 G(\vec{R}, \vec{r}) = \delta(\vec{R}, \vec{r}), \quad (13)$$

and gives  $G(\vec{R}, \vec{r}) = 0$  for  $\vec{R}$  on the boundary. Thus the quantity appearing in the exponent of (11) appears to involve  $\lim_{\vec{R} \rightarrow \vec{r}} G(\vec{R}, \vec{r})$ , which does not exist. However, this same difficulty occurs in electrostatics in the evaluation of the electrostatic energy of a unit point charge

at position  $\vec{r}$  near a conducting boundary:  $G(\vec{R}, \vec{r})$  is the potential at point  $\vec{R}$  caused by the charge, but to calculate the energy we must remove the self-energy of the point charge. In the present context this suggests that we should replace  $G$  by

$$\tilde{G}(\vec{r}) = \lim_{\vec{R} \rightarrow \vec{r}} [G(\vec{R}, \vec{r}) + \frac{1}{2\pi} \ln |\vec{R} - \vec{r}|], \quad (14)$$

and then write

$$m(\vec{r}) = e^{-\frac{1}{2g} \tilde{G}(\vec{r})}. \quad (15)$$

This subtraction can be viewed as a modification of the action (6), in which the fields  $\theta$  become "normal-ordered" [1]. What has been subtracted in Eq.(14) is independent of  $\vec{r}$  – it is an (infinite) constant. The result is that  $\tilde{G}(\vec{r})$  is finite throughout the domain but diverges to  $-\infty$  at the boundary, thus returning the boundary behavior (5) for  $m(\vec{r})$ . We see that by solving an electrostatics problem we can obtain the order parameter for the Gaussian model defined on the same geometry.

We now argue that this result describes the critical magnetization profile for any model that can be studied by conformal field methods. The argument is as follows: we can match the order parameter profile for the Gaussian model in the case of the half-plane geometry (Eq. 5) to that of any given critical model by choosing

$$\frac{1}{4\pi g} = \Delta, \quad (16)$$

since for this case  $\tilde{G}(\vec{r}) = \frac{1}{2\pi} \ln |2y|$  – the part of the Green function due to the "image charge." But then the conformal transformation rule (1) does not depend on any property of the ordering field other than the conformal dimension  $h$ , or equivalently the exponent  $\Delta$ . Thus we can conclude that any critical model in two dimensions will have the same order parameter profile as its matching Gaussian model, at least for all boundary geometries that are related to the half-plane by a conformal transformation. In view of the simple way that  $g$  enters into Eq. (15), this result can be restated to say that the order parameter profile for these cases can be written in the form (5).

Here are some examples:

\*The disk with spins fixed at the value of +1 on the boundary:

$$< m(r) > = C |A - \frac{r^2}{A}|^{-\Delta}. \quad (17)$$

Here  $A$  is the radius of the disk and  $r$  is the distance from the center of the disk. This expression is valid [5] for both  $r < A$  and  $r > A$ .

\*The infinite strip  $\vec{r} = (x, y)$  with  $0 \leq y \leq W$ , with spins fixed at +1 on the boundaries  $y = 0$  and  $y = W$ :

$$< m(\vec{r}) > = C (\sin \pi \frac{y}{W})^{-\Delta}. \quad (18)$$

The derivation of this expression is discussed in Appendix A.

\*The rectangle  $-\frac{L}{2} \leq x \leq \frac{L}{2}$ ,  $0 \leq y \leq W$ , with spins on all boundaries fixed at the value +1:

$$\langle m(w) \rangle = C \left[ \frac{\text{Im}[\text{sn}(\frac{2K}{L}w)]}{|\text{cn}(\frac{2K}{L}w)\text{dn}(\frac{2K}{L}w)|} \right]^{-\Delta}, \quad (19)$$

where  $w = (x + iy)$  is a complex variable defined on the rectangle, and sn, cn, dn are the Jacobian elliptic functions [6]. The aspect ratio of the rectangle enters through the modulus of the elliptic functions: the quarter periods  $K$  and  $K'$  are related by  $K'/K = 2W/L$ . The derivation of this result is given in appendix A. Even though elliptic functions are a little less well known than the functions that appear in Eqs. (17) and (18), the rectangular geometry is might be easier to study numerically, and the expression (19) is easily evaluated.

Common to all the problems mentioned above is that the boundaries are conformal images of the real axis. They can also be obtained [4] by conformal mapping from the half-plane, transforming Eq. (4) by means of Eq. (1).

The order parameter profile for the Gaussian model on an infinite strip with opposed boundaries (spin +1 on one side, spin -1 on the other) can be found by an extension of the method. The Gaussian field  $\theta$  is divided into two parts:

$$\theta(\vec{r}) = \theta_0(\vec{r}) + \theta_1(\vec{r}), \quad (20)$$

where  $\theta_1(\vec{r})$  is a fluctuating field that vanishes on the boundary while  $\theta_0(\vec{r}) = \pi y/W$  is the solution to Laplace's equation with the opposed boundaries. Partial integration then shows

$$S = \frac{1}{2}g \int (|\vec{\nabla}\theta_0|^2 + |\vec{\nabla}\theta_1|^2) d^2r, \quad (21)$$

so that  $\theta_1$  is not coupled to  $\theta_0$  in the statistical averaging. It follows that

$$m_{+-}(\vec{r}) = \langle \text{Re}e^{i(\theta_0(\vec{r}) + \theta_1(\vec{r}))} \rangle = m_{++}(\vec{r}) \cos \pi y/W, \quad (22)$$

where  $m_{++} = m_1^\Delta$  is the profile for the case that the boundary conditions are the same on opposite boundaries, which we have already considered. This result has been previously obtained [7] by means of a conformal field theory argument. The argument above now implies that a universal prescription can be given for the magnetization profile in a region whose boundary is an image of the real axis, with boundary conditions that change from + to -.

The Gaussian model is known to give the incorrect two-point correlation function for the Ising model [2], and so despite the successes reported above, we should not assume that the Gaussian model correctly reproduces the magnetization profile for all models in *all* boundary conditions. A counterexample is the case of the Ising model

with spins fixed at +1 on two ends of a cylinder (i.e. a rectangle with periodic boundary conditions joining a pair of sides). Since this geometry cannot be related to the half-plane by a conformal transformation (the boundary is not in any sense connected), the chain of logic that allowed us to identify order parameter profiles for the Gaussian model with those for nontrivial models is broken. The Gaussian model solution for this case is given in Appendix A, with the result

$$\langle m(x, y) \rangle = |\theta_1(\frac{2\pi i}{L}y) \exp(-\frac{4\pi}{L^2\tau}y^2)|^{-\Delta}, \quad (23)$$

where  $\theta_1$  is the theta function [6] of nome  $q = \exp(-2\pi W/L)$  and  $\tau = 2W/L$ . As will be seen below, simulations do not support this form well, and indicate that the Ising model magnetization is better represented by

$$\langle m(x, y) \rangle = \frac{|\theta_2(\frac{\pi i}{L}y)|^{\frac{1}{2}} + |\theta_3(\frac{\pi i}{L}y)|^{\frac{1}{2}}}{|\theta_1(\frac{2\pi i}{L}y)|^{\frac{1}{8}}}. \quad (24)$$

In comparing these, please note that  $\Delta = \frac{1}{8}$  for the Ising model. The logic leading to Eq. (24) is explained in Appendix B.

### III. NUMERICAL SIMULATIONS

We tested the predictions of conformal field theory by simulating the Ising model and the bond percolation problem on the square lattice.

For the Ising model we used the Swendsen-Wang Monte Carlo algorithm [8]. For each simulation the number of Monte Carlo steps per site was  $10^6$ . In each simulation the intial configuration was all spins at the state of +1. The undetermined constant  $C$  was used as a fitting parameter.

The percolation threshold for the bond percolation problem on the square lattice is  $p_c = \frac{1}{2}$ . We evaluated  $m(\vec{r})$  by averaging  $10^6$  random bond assignments.

\**Disk geometry.* We cut a disk from a piece of square lattice with unit lattice constant, defined by the sites for which  $|\vec{r}| < A$ . Sites outside this disk were in frozen state: all "spin +" for the Ising model or "connected to the boundary" for percolation. We averaged the magnetization over all directions to obtain  $m(r)$ . The results are shown in Figure 1, which is a graph of  $\ln m(r)$  versus  $\ln(A - r^2/A)$ . The data is expected to fall on straight lines of slope  $-\Delta$ , according to Eq. (17). Dashed lines having the appropriate slopes have been drawn in for comparison. Since the simulations were done for lattice systems and the theory is derived for a continuum model, there can be a discrepancy close to the boundary. In our simulations, the boundary is rough at the lattice scale, and in most directions is slightly more than  $A$  lattice spacings from the center. Therefore we allowed the value used for

$A$  in the fitting to be slightly larger than the (integer) value used to define the disk, chosen so as to eliminate curvature that would otherwise appear at the left edge of Figure 1 (order close to the disk boundary). We found the optimal value to be  $A = \text{radius} + 0.7$  for the Ising model and  $A = \text{radius} + 0.5$  for percolation. By fitting the data for the disks of three different radii and finding the average slope we get  $\Delta = 0.1234 \pm 0.0005$  for the Ising model, and  $\Delta = 0.1036 \pm 0.0002$  for percolation. The theoretical prediction from Eq. (17) is  $\Delta = 0.125$  for the Ising model, and  $\Delta \approx 0.10417$  for percolation. Thus this seems to be a viable way to determine  $\Delta$ .

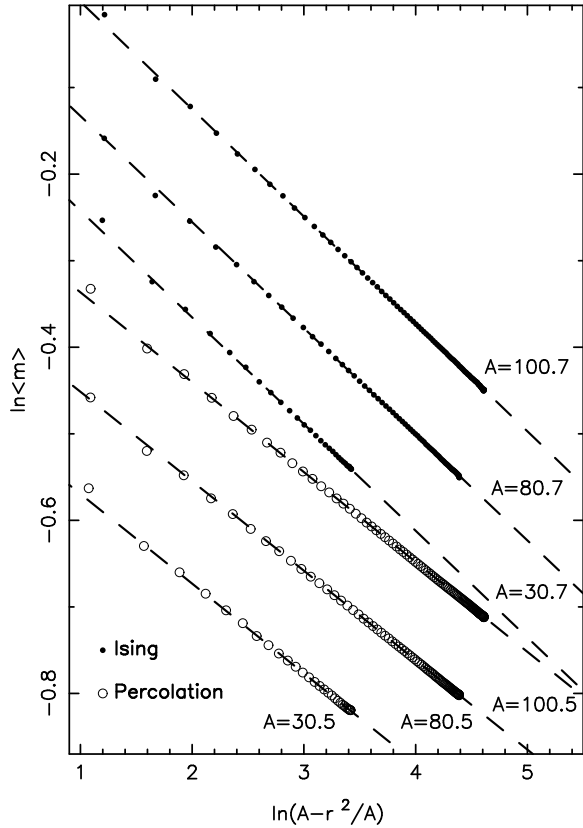


FIG. 1. Linear fits for the Ising model and percolation on the disk

\*Ising model on infinite periodic strip with ++ boundaries. In a simulation we can work only with finite strips. A rectangle ( $0 \leq x \leq L, 0 \leq y \leq W$ ) which is periodic in  $x$  direction approximates an infinite strip really well if the periodic dimension (in our case  $L$ ) is greater or equal than the dimension in the nonperiodic direction (in our example  $W$ ). The results for the case  $L = W$  are shown in Fig. 2. The spins on the boundary  $y=0$  and  $y=W$  were fixed at the value of +1.

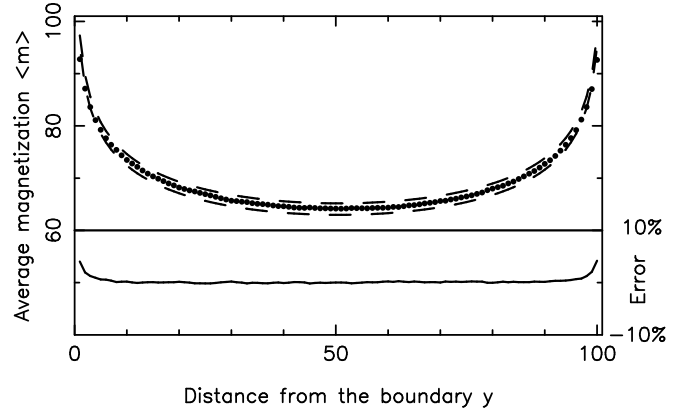


FIG. 2. Average value of magnetization as a function of the distance from the boundary for  $L=W=100$ .

The dashed lines are the theoretical curve

$$\langle m(r) \rangle = C(\sin \pi \frac{y}{W})^{-\frac{1}{8}}, \quad (25)$$

obtained from Eq. (18), displaced by a small constant amount upwards and downwards, since otherwise the theory and data would greatly overlap. The lower part of this figure is a separate graph of the same information, now presented as the relative error  $ER = 100 * (m_{th} - m_{exp})/m_{exp}$ . We will use this format in most of our figures.

\*Ising model on infinite strip with +- boundaries. As above, we approximate the infinite strips with rectangles ( $0 \leq x \leq L, 0 \leq y \leq W$ ),  $L \geq W$ . The results for the case  $L=W=100$  are shown in Fig. 3.

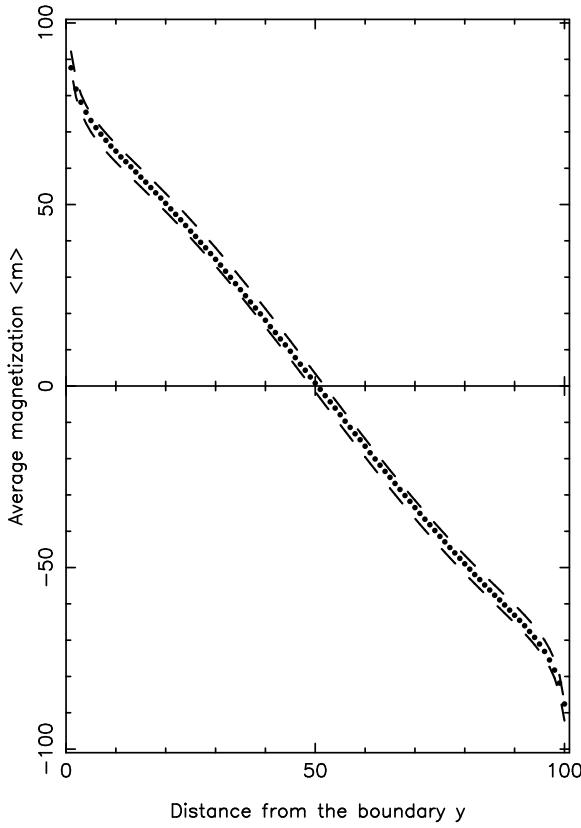


FIG. 3. Average value of magnetization as a function of the distance from the positive boundary for  $L=W=100$ .

The spins on the boundary  $y=0$  were kept at the value of +1, while the spins on the boundary  $y=W$  were fixed at the value of -1. The dashed lines are the theoretical curve:

$$\langle m(r) \rangle = C \left( \sin \pi \frac{y}{W} \right)^{-\frac{1}{8}} \cos \pi \frac{y}{W}, \quad (26)$$

obtained from Eq. (22), displaced as before.

\*Percolation on infinite periodic strip. As in the Ising model, we approximate the infinite strip with a square ( $0 \leq x \leq 100, 0 \leq y \leq 100$ ) which is periodic in  $x$  direction. The results are shown in Fig. 4.

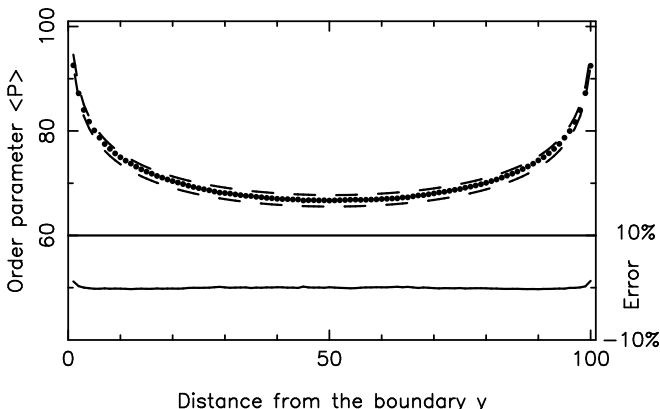


FIG. 4. Order parameter as a function of the distance from the boundary for a periodic square 100x100.

The dashed lines are the theoretical curve:

$$\langle m(r) \rangle = C \left( \sin \pi \frac{y}{W} \right)^{-\frac{5}{48}}. \quad (27)$$

\*Ising model on rectangle. The rectangle ( $0 \leq x \leq L, 0 \leq y \leq W$ ) was defined by spins fixed at the value of +1 on all boundaries. The average magnetization was measured as a function of the distance from the boundary  $y=0$ . The results for the square  $(L,W)=(100,100)$  are shown in Fig. 5 and in Fig. 6. The magnetization in Fig. 5 was measured along the line ( $x=10, y$ ) while in Fig. 6 the measurement was along the line ( $x=50, y$ ).

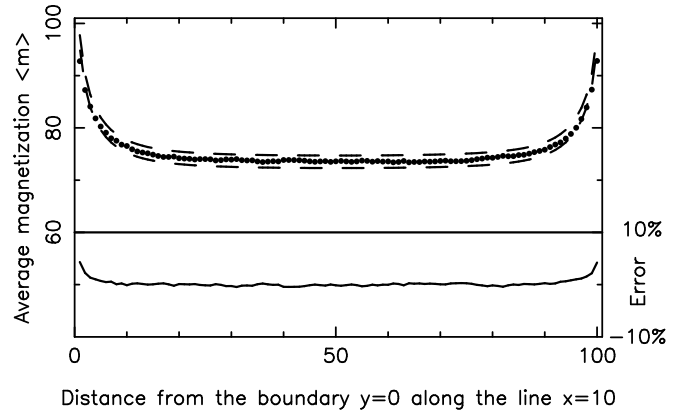


FIG. 5. Average value of magnetization along the line ( $x=10, y$ )

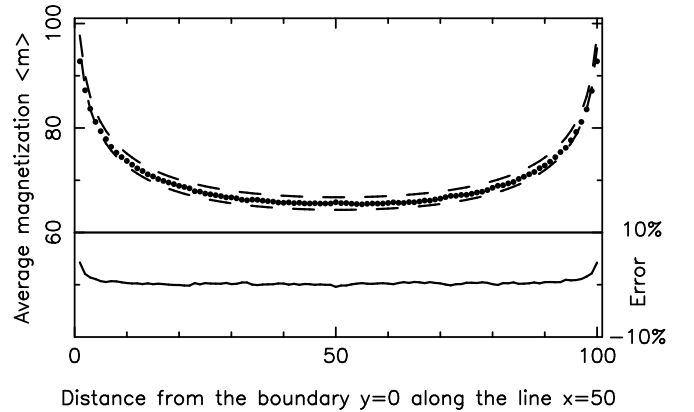


FIG. 6. Average value of magnetization along the line ( $x=50, y$ )

The dashed lines are the theoretical curve:

$$\langle m(w) \rangle = C \left[ \frac{\text{Im}[\text{sn}(\frac{2K}{L}w)]}{\text{cn}(\frac{2K}{L}w) \text{dn}(\frac{2K}{L}w)} \right]^{-\frac{1}{8}}, \quad (28)$$

obtained from Eq. (19).

\*Percolation on rectangle. The rectangle is ( $0 \leq x \leq 100, 0 \leq y \leq 100$ ). The order parameter is given as a

function of the distance from the boundary  $y = 0$ . The results along the line ( $x = 10, y$ ) are given in Fig. 7 while in Fig. 8 the measurement was along the line ( $x = 50, y$ ).

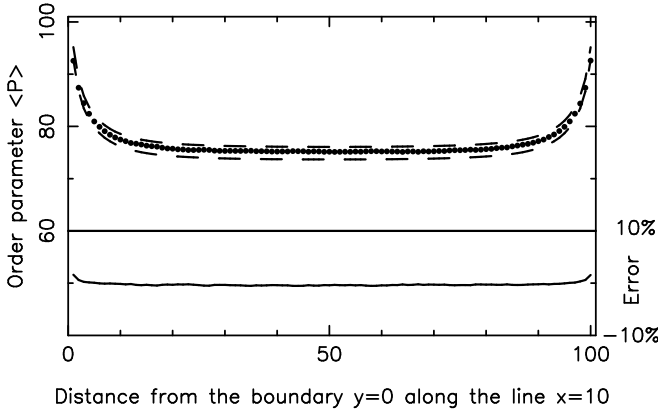


FIG. 7. Order parameter along the line ( $x=10, y$ )

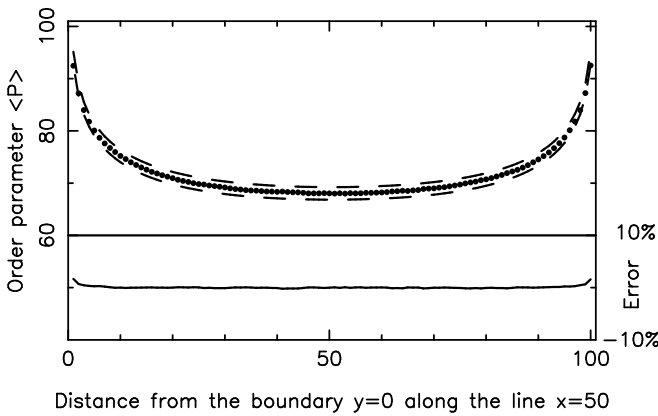


FIG. 8. Order parameter along the line ( $x=50, y$ )

The dashed lines are the theoretical curve:

$$\langle m(w) \rangle = C \left[ \frac{\operatorname{Im}[\operatorname{sn}(\frac{2K}{L}w)]}{\operatorname{cn}(\frac{2K}{L}w) \operatorname{dn}(\frac{2K}{L}w)} \right]^{-\frac{5}{48}}. \quad (29)$$

\*Ising model on the periodic rectangle. We used the rectangle ( $0 \leq x \leq L, 0 \leq y \leq W$ ) periodic in the  $x$  direction, with the spins kept at the value of +1 on the boundaries  $y=0$  and  $y=W$ . As we have seen above, the case  $L \geq W$  resembles the infinite periodic strip. Here we will consider  $L < W$ . In Fig. 9 we show the average value of magnetization for rectangle  $L=80, W=101$ . In Fig. 10 the rectangle is  $L=40, W=101$ .

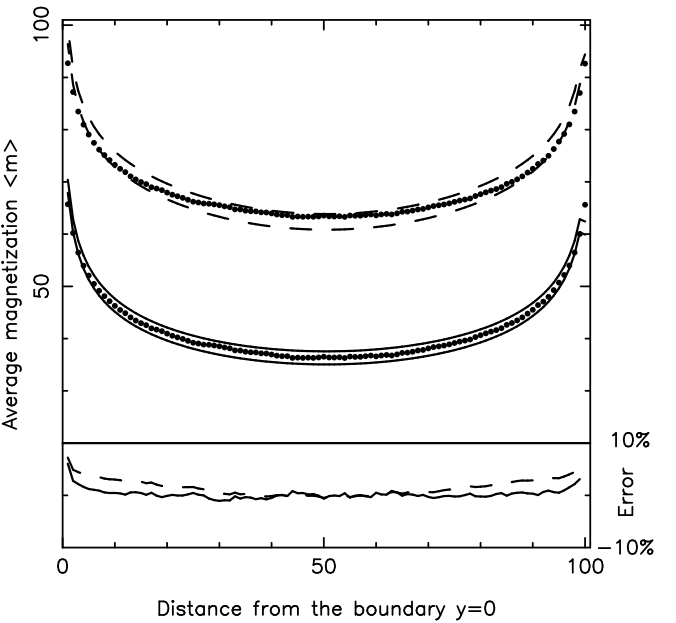


FIG. 9. Average value of magnetization for the (80,101) rectangle. The data is displayed twice, with a vertical displacement. The upper set of lines compares the magnetization to the prediction (23) based on the Gaussian model. The lower set is Eq. (24), supplied by conformal field theory.

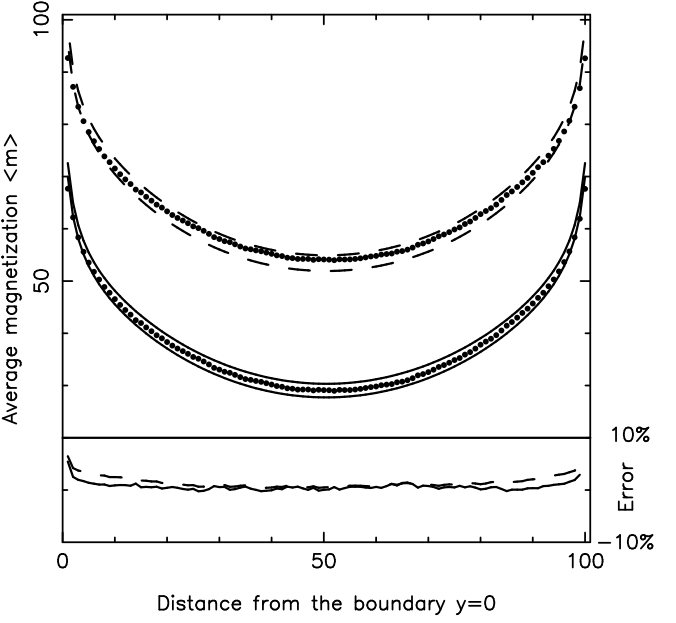


FIG. 10. Average value of magnetization for the (40,101) rectangle. Same comparisons as in figure 9.

In the lower part of the figure, the full line is the relative error for the conformal field theory prediction while the Gaussian model error is represented by the dashed line. The same convention will be used in Fig. 11 and in Fig. 12. The agreement between the data and the predictions of the Gaussian model is not very good; Eq. (24)

coming from conformal field theory does much better.

\*Percolation on the periodic rectangle. The position of percolation theory in conformal field theory is as yet unclear: it apparently is not a unitary minimal model, and it is not known whether there is a differential equation to which  $m(\vec{r})$  is a solution. In view of the failure of the Gaussian model to describe the magnetization profile of the Ising model, we have no theory for this case. We have chosen to give the same analysis as was done for the Ising model, changing only the exponent  $\Delta$ . Thus the top set of curves in Figures 11 and 12 compare the behavior of the percolation order parameter to the Gaussian model (23), while the lower set compare the same data to

$$\langle m(x, y) \rangle = \left( \frac{|\theta_2(\frac{\pi i}{L}y)|^{\frac{1}{2}} + |\theta_3(\frac{\pi i}{L}y)|^{\frac{1}{2}}}{|\theta_1(\frac{2\pi i}{L}y)|^{\frac{1}{8}}} \right)^{\frac{5}{6}}, \quad (30)$$

which is related to the Ising model expression (24) through the universality hypothesis Eq. (5). There's no reason for this to work! But it seems to agree with the data!

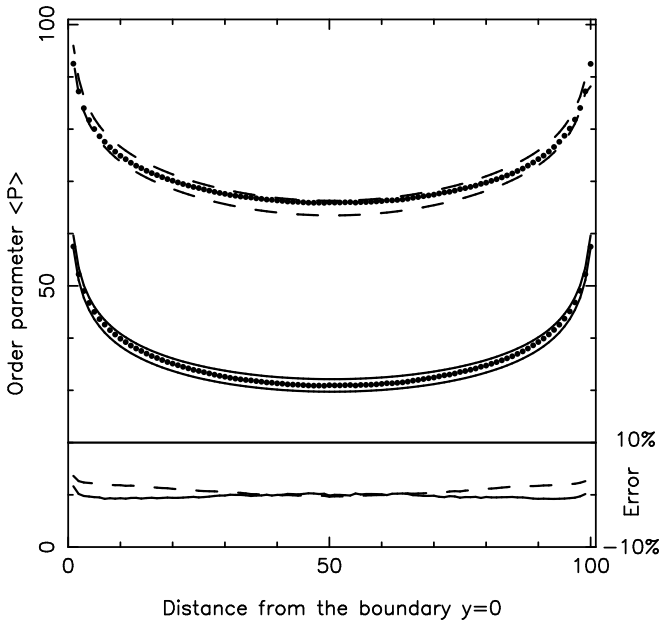


FIG. 11. Order parameter for the (81,101) rectangle

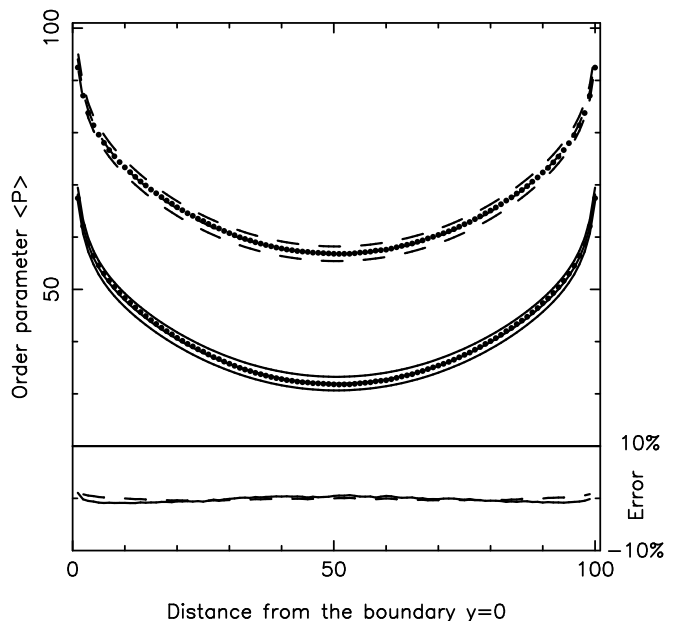


FIG. 12. Order parameter for the (41,101) rectangle

#### IV. PLANAR SPIN MODEL

The planar spin model consists of unit spins that can point in any direction in the x-y plane. The Hamiltonian for this model can be written as

$$H = -J \sum_{\langle i,j \rangle} \cos(\theta_i - \theta_j), \quad (31)$$

where the sum is over the nearest neighbors.  $\theta_i$  is the angle the  $i$  th spin makes with the x axis.

The model undergoes a Kosterlitz-Thouless (KT) transition [13–15] at the critical temperature  $T = T_c$ . Below this temperature there is algebraic order at all temperatures, implying a lack of a length scale and thus conformal invariance; unlike three dimensional phase transitions, however, the exponent  $\eta$  depends on temperature. We determined  $m(\vec{r})$  by means of simulations on a disk of radius 100, with  $\theta = 0$  on the boundary (i.e. the spins on the boundary are constrained to point in the x direction), using Wolff's algorithm [16]. After the equilibration we performed  $10^6$  Monte Carlo steps per site. By using  $\langle m(r) \rangle$  obtained from numerical simulations we can find  $\eta$ , since Eqs.(3) and (17) imply

$$\ln \langle m(r) \rangle = -\frac{\eta}{2} \ln(A - \frac{r^2}{A}) + \text{constant}. \quad (32)$$

Linear regression was used to determine the slopes of the lines in Fig. 13, which gives the exponent  $\eta(T)$ .

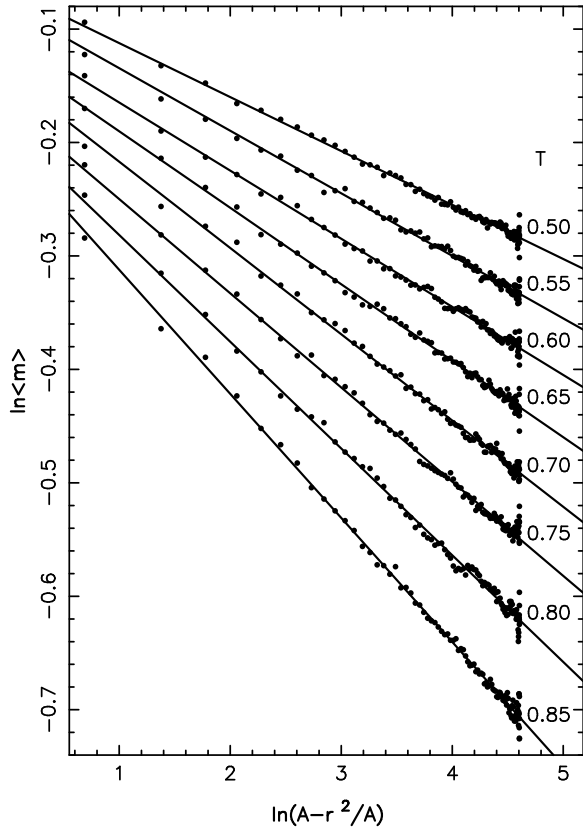


FIG. 13. Linear fits for temperatures  $0.85J$ ,  $0.80J$ ,  $0.75J$ ,  $0.70J$ ,  $0.65J$ ,  $0.60J$ ,  $0.55J$ ,  $0.50J$

Our results are given in Table I:

T	0.85J	0.80J	0.75J	0.70J	0.65J	0.60J	0.55J	0.50J
$\eta$	0.2187	0.1882	0.1660	0.1521	0.1348	0.1201	0.1103	0.0951

TABLE I. Critical exponent as a function of temperature

According to Kosterlitz-Thouless theory [17], the long wavelength spin fluctuations are described by the Hamiltonian (32) with a renormalized coupling constant  $J(T)$ , given by

$$J(T)/T = \frac{2}{\pi} - (\text{constant}) \sqrt{\frac{T - T_C}{T_C}}, \quad (33)$$

where the constant is determined by the core energy for a vortex. This determines the temperature dependence of  $\eta = T/2\pi J$ , so that close to the Kosterlitz-Thouless transition

$$[\frac{1}{4} - \eta(T)]^2 \approx \frac{T_C - T}{T_C}, \quad (34)$$

implying that  $\eta$  approaches its critical value by a square-root cusp. We note that many of the previous studies [15,18] of  $\eta(T)$  have incorrectly assumed a linear dependence.

Figure 14 shows the analysis of the data from Table I.

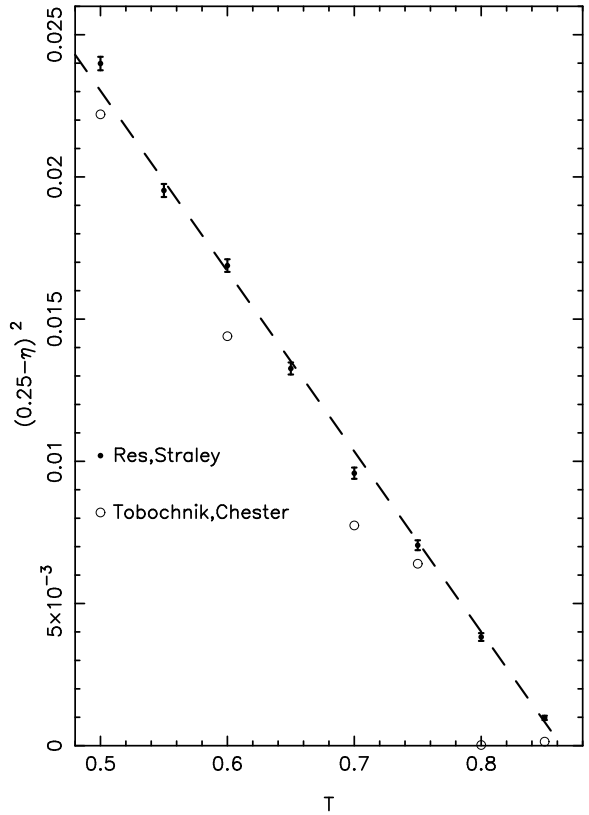


FIG. 14. Data comparison

The points follow a straight line as predicted by eq.(34). The critical temperature is given by the intersection of this line with the temperature axis and is found to be

$$T_C/J = 0.863 \pm 0.009. \quad (35)$$

In Fig. 14 we also plotted the results obtained by Tobochnik and Chester (TC) [15]. We notice that their data consistently fall below our line, but are consistent with it. TC analyzed their data using a linear extrapolation to obtain  $T_C/J = 0.89 \pm 0.01$ . Our reanalysis of their data indicates a lower value. We also quote the estimates for  $T_C$  obtained by some other authors: Weber and Minnhagen [19] give  $T_C/J = 0.887 \pm 0.002$  while Olsson [23] finds  $T_C/J = 0.8922(2)$ .

The results obtained by computer simulations in the critical region are affected by the finite size effects - one is trying to obtain predictions for the infinite system by simulating a finite system. Our approach avoids this problem because the theory says that the critical exponent  $\eta$  for the model defined on a disk must in principle be equal to the exponent  $\eta$  for the infinite system. The only approximation involved is the passage from a discrete system to continuum.

## V. SUMMARY

In this work, we studied the magnetization of the Ising model and percolation defined on finite geometries. We derived the order parameter for rectangle by using conformal symmetry. We showed how the results previously obtained by using conformal field theory can be obtained by studying a simple Gaussian model. We numerically studied order parameter in various geometries by using Monte Carlo methods and compared analytical results with the outcome of our simulations.

## VI. APPENDIX A

To determine the order parameter for the model defined on an infinite strip ( $x, 0 \leq y \leq W$ ) with spins fixed at the value of +1 on the boundaries, we find the electrostatics Green function for the infinite strip with Dirichlet boundary conditions:

$$G(Z, z) = \frac{1}{2\pi} \left( \ln \left| \sin \frac{\pi|Z - z^*|}{2W} \right| - \ln \left| \sin \frac{\pi|Z - z|}{2W} \right| \right), \quad (36)$$

where  $z = x + iy$  is the complex representation of the plane, and  $z^* = x - iy$  is the position of an image of  $z$  [12]. This result can be obtained by conformal mapping from the half-plane; or from the observation that Eq.(36) has logarithmic singularities of opposite signs at the positions of all images (in the two boundaries) of  $z$  and is a solution to the two-dimensional Laplace problem elsewhere, since it can be written as the sum of a function of  $Z$  and a function of  $Z^*$ . The non-singular part of the Green function is then

$$\tilde{G}(\vec{r}) = \frac{1}{2\pi} \ln \left( \sin \frac{\pi y}{W} \right). \quad (37)$$

Eq. (15) then gives the result quoted in text.

The magnetization profile for a rectangle can be found using a conformal mapping, as follows: The semi-infinite complex plane  $z = (x, y \geq 0)$  is mapped onto the rectangle  $(-\frac{L}{2} \leq u \leq \frac{L}{2}, 0 \leq iv \leq iW)$  in the complex plane  $w = (u, iv)$  by the Schwarz-Christoffel transformation [9,1,4]

$$w(z) = -\frac{L}{2K} \int_0^z g(z') dz', \quad (38)$$

where

$$g(z) = \frac{1}{\sqrt{1 - k^2 z^2}} \frac{1}{\sqrt{1 - z^2}}, \quad (39)$$

with

$$K = \int_0^1 |g(x')| dx', \quad (40)$$

$$K' = \int_1^a |g(x')| dx'. \quad (41)$$

The ratio of  $K$  and  $K'$  is related to the nome  $q$  of the Jacobian elliptic functions [6]

$$q = e^{-\pi \frac{2W}{L}}. \quad (42)$$

The inverse of the function  $w(z)$  is the Jacobian elliptic function  $z = sn(\frac{2K}{L}w)$ , which implicitly depends [6] on the nome  $q$ . Then we can put (4) and (38) into Eq. (1), noting that  $y = Im[sn(\frac{2K}{L}w)]$ , to obtain

$$\langle m(w) \rangle = C \left| \frac{Im[sn(\frac{2K}{L}w)]}{\sqrt{1 - k^2 sn^2(\frac{2K}{L}w)} \sqrt{1 - sn^2(\frac{2K}{L}w)}} \right|^{-\Delta}. \quad (43)$$

We use the relations between Jacobi elliptic functions  $sn$ ,  $cn$ ,  $dn$  [6] to obtain Eq. (19).

This result can also be obtained through the connection with the Gaussian model. This requires finding the Dirichlet Green function for the rectangle, which can be found by the method of images. The images of the point  $\vec{r}$  lie on four rectangular Bravais lattices, and the Green function itself is an infinite sum of the corresponding logarithmic terms. The sum can be evaluated by observing that  $\exp(2\pi G(\vec{R}, \vec{r}))$  has only simple poles and zeroes, which form periodic arrays, and thus it is a function of elliptic type [6]. Inspection then gives

$$\exp(2\pi G(\vec{R}, \vec{r})) = \frac{\theta_1(\pi \frac{Z-z}{2L}) \theta_1(\pi \frac{Z-z''}{2L})}{\theta_1(\pi \frac{Z-z'}{2L}) \theta_1(\pi \frac{Z-z'''}{2L})}, \quad (44)$$

where  $\theta_1$  is the theta function [11,6],  $Z$  is the complex representation of  $\vec{R}$ , and the  $z$ 's are the complex representations of  $\vec{r}$  and the image points  $z' = z^*$ ,  $z'' = L - z$ ,  $z''' = L - z^*$ . The resulting expression for the order parameter profile is

$$\langle m(x, y) \rangle = \left| \frac{\theta_2(\frac{\pi x}{L}) \theta_1(\frac{i\pi y}{L})}{\theta_2(\pi \frac{x+iy}{L})} \right|^{-\Delta}. \quad (45)$$

This representation is equivalent to the one used above, but is easier to evaluate numerically, since the series representations [6] for the theta functions converge extremely rapidly.

The Dirichlet Green function for a  $L \times W$  rectangle with fixed boundary conditions on two sides and periodically connected along the other two has logarithmic singularities at  $Z = z + mL + inW$ , and logarithmic singularities of opposite sign at  $Z = z^* + mL + inW$ , where  $z^* = x - iy$ . This behavior is reproduced by the function

$$G(Z, z) = -\frac{1}{2\pi} \ln \left| \frac{\theta_1(\pi \frac{Z-z}{L}) e^{\frac{\pi}{L^2\tau}(Z-z)^2}}{\theta_1(\pi \frac{Z-z^*}{L}) e^{\frac{\pi}{L^2\tau}(Z-z^*)^2}} \right|. \quad (46)$$

Here  $\tau = 2W/L$  specifies the shape of the rectangle. We take the limit  $Z \mapsto z$  as we did in the case of nonperiodic rectangle and obtain eq. (23).

## VII. APPENDIX B

According to conformal field theory [1], the N-point correlation functions of many critical models can be found by solving a differential equation originating in the algebra of the operators corresponding to the fields. In many cases, the correlation function factors into a product of holomorphic (depending on  $z$ ) and antiholomorphic ( $z^*$ ) parts, or a sum of a small number of such terms. Cardy [20] has given a prescription for introducing a straight homogeneous boundary into this formalism. In effect, the N-point function is found by solving the  $2N$ -point differential equation for the holomorphic part, and then evaluating this with the second set of points at the image position (i.e.  $z_{N+1} = z^*$  if the boundary is the real axis). Since the differential equations are of higher than first order, there are several solutions to choose from, and the choice is determined by the boundary condition (e.g. Dirichlet) desired.

The problem we wish to consider is the rectangle with Dirichlet boundary conditions on two opposite edges and periodic continuation on the other two edges. This is equivalent to a finite length cylinder with Dirichlet boundary conditions on the ends, or to a torus that is cut by a single Dirichlet seam.

The differential equation appropriate for the Ising model spin operator on a torus has been given by Eguchi and Ooguri [21], and the solutions for the two-point function are given by Di Francesco et al. [22]. They all have the form

$$\langle \sigma \sigma \rangle = \frac{[\theta_\nu(\frac{z_1-z_2}{2})]^{\frac{1}{2}}}{[\theta_1(z_1-z_2)]^{\frac{1}{8}}}, \quad (47)$$

where  $\theta_\nu$  ( $\nu = 2, 3, 4$ ) are the theta functions with the periodicity of the torus. The combination  $\langle \sigma \sigma \rangle_2 + \langle \sigma \sigma \rangle_3$  has the desired periodicity in  $\text{Im } z$ . We then follow Cardy by evaluating this with  $z_1 = z$ ,  $z_2 = z^*$ .

into the sphere interior, so that Eq. (17) is also valid. This still isn't very interesting, because the general case of Eq. (3) is  $\Delta = \frac{1}{2}(d-2+\eta)$ , where  $\eta$  is expected to be small.

- [6] M. Abramowitz, I. A. Stegun, *Handbook of Mathematical Functions*, (Dover, New York, 1964), Chapter 16.
- [7] T. W. Burkhardt, I. Guim, Phys. Rev. B **53**, 2080 (1987).
- [8] R. H. Swendsen, J.-S. Wang, Phys. Rev. Lett. **58**, 86 (1987).
- [9] R. V. Churchill, J.W. Brown, *Complex Variables and Applications*, (McGraw-Hill, 1990).
- [10] D. Stauffer, A. Aharony, *Introduction to Percolation Theory*, (Taylor & Francis, 1994).
- [11] E. T. Whittaker, G. N. Watson, *A Course of Modern Analysis*, (Cambridge University Press, 1962)
- [12] J. D. Jackson, *Classical Electrodynamics*, (Wiley, 1975)
- [13] J. M. Kosterlitz, D. J. Thouless, J. Phys. C **6**, 1181(1973).
- [14] J. M. Kosterlitz, J. Phys. C **7**, 1046(1974).
- [15] J. Tobochnik, G. W. Chester, Phys. Rev. B **20**, 3761(1979).
- [16] U. Wolff, Phys. Rev. Lett. **62** 361(1989).
- [17] P. M. Chaikin, T. C. Lubensky *Principles of Condensed Matter Physics*, (Cambridge University Press, 1995).
- [18] J. F. Fernández, M. F. Ferreira, and J. Stankiewicz, Phys. Rev. B **34**, 292 (1986).
- [19] H. Weber, P. Minnhagen, Phys. Rev. B **37**, 5986 (1988).
- [20] J. L. Cardy, Nucl. Phys. **B240** [FS12] 514 (1984).
- [21] T. Eguchi and H. Ooguri, Nucl. Phys. **B282**, 308 (1987).
- [22] P. Di Francesco, H. Saleur, and J.-B. Zuber, Nucl. Phys. **B290** [FS20], 527 (1987).
- [23] P. Olsson, Phys. Rev. Lett. **73**, 3339 (1994).

---

- [1] P. Di Francesco, P. Mathieu, D. Sénéchal, *Conformal Field Theory*, (Springer-Verlag, 1997).
- [2] J. Cardy, *Scaling and Renormalization in Statistical Physics*, (Cambridge University Press, 1996).
- [3] H. Gould, J. Tobochnik, *An Introduction to Computer Simulation Methods*, (Addison-Wesley, 1996).
- [4] T. W. Burkhardt, E. Eisenriegler, J. Phys. A **18**, L83(1985).
- [5] Higher-dimensional systems can also be conformally invariant at the critical point. The set of conformal transformations is very small, so that there are few consequences; but we note that Eq. (4) continues to describe the decay of correlations near an ordered boundary, and that there is a conformal transformation of the half-space